(Fig. 1). The curve fit the data well at r = 0.95, ED_{50} = 4.6 ng/ml.

Discussion

The present results demonstrated the time course of fluvoxamine in the living human brain expressed by 5-HTT occupancy. The dissociation of the elimination time of fluvoxamine between brain concentration and plasma concentration has been reported in a magnetic resonance spectroscopy (MRS) study.[8] The time course of the elimination of fluvoxamine from the brain was reported to be fitted to a one-exponential curve. However, the MRS technique might measure the total concentration in the brain including free and non-specific binding, and 5-HTT occupancy might reflect the concentration at 5-HTT. Theoretically, the time course of 5-HTT occupancy does not fit to linear or exponential function.[9]

About 80% 5-HTT occupancy was reported during treatment with clinical doses of SSRIs.[3] However, the threshold of 5-HTT occupancy for the treatment of depression has not been clearly determined, and it is still unresolved whether high 5-HTT occupancy should be maintained or a transient high occupancy is enough for treatment. Some reports suggested that "drug holidays" would reduce SSRI-induced sexual dysfunction.[10] But discontinuation syndrome of SSRIs, such as insomnia, confusion, dizziness, headaches and gastrointestinal upset,[11] has been reported to more likely occur

in patients with shorter plasma half-life SSRIs.[12] Investigation of the time course of 5-HTT occupancy would provide new insight into the pathophysiology of the discontinuation syndrome and help to determine the appropriate drug administration interval.

Significant regional differences in 5-HTT occupancy by fluvoxamine were not observed in this study. The test - retest study of BP values by MRTM2 showed good reproducibility in all the measured regions, and the results were in agreement with previous reports.[13]

The relationship between the plasma concentration of fluvoxamine and 5-HTT occupancy in this time-course study was shown to follow the law of mass action. The ED_{50} value (4.6 ng/ml) in this time-course study was not so different from the previous study (4.19 ng/ml) using a different radioligand [^{11}C]McN5652.[2] This indicated that the time course of 5-HTT occupancy could be estimated from the plasma pharmacokinetics and ED_{50} value. However, the time course of 5-HTT occupancy was investigated by a single administration of fluvoxamine in healthy volunteers, the results of this study were preliminary, and further studies using repeated administrations to patients will be necessary.

References

1. Owens MJ, Morgan WN, Plott SJ, et al. Neurotransmitter receptor and transporter binding profile of antidepressants and their metabolites. J Pharmacol Exp Ther 1997;283:1305-22.

2. Suhara T, Takano A, Sudo Y, et al. High levels of serotonin transporter occupancy with low-dose clomipramine in comparative occupancy study with fluvoxamine using positron emission tomography. Arch Gen Psychiatry 2003;60:386-391.

3. Meyer JH, Wilson AA, Sagrati S, et al. Serotonin transporter occupancy of five selective serotonin reuptake inhibitors at different doses: an [^{11}C]DASB positron emission tomography study. Am J Psychiatry 2004;161:826-35.

4. Ginovart N, Wilson AA, Meyer JH, et al. [^{11}C]DASB, a tool for in vivo measurement of SSRI-induced occupancy of the serotonin transporter: PET characterization and evaluation in cats. Synapse 2003;47:123-33.

5. Wilson AA, Ginovart N, Schmidt M, et al. Novel radiotracers for imaging the serotonin transporter by positron emission tomography: synthesis, radiosynthesis, and in vitro and ex vivo evaluation of ^{11}C-labeled 2-(phenylthio)araalkylamines. J Med Chem 2000;43:3103-10.

6. Yasuno F, Hasnine AH, Suhara T, et al. Template-based method for multiple

volumes of interest of human brain PET images. Neuroimage 2002;16:577-86.

7. Ichise M, Liow JS, Lu JQ, et al. Linearized reference tissue parametric imaging methods: application to [^{11}C]DASB positron emission tomography studies of the serotonin transporter in human brain. J Cereb Blood Flow Metab 2003;23:1096-112.

8. Strauss WL, Layton ME, Dager SR. Brain elimination half-life of fluvoxamine measured by ^{19}F magnetic resonance spectroscopy. Am J Psychiatry 1998;155:380-384.

9. Takano A, Suhara T. The necessary parameters for estimating the time-course of receptor occupancy. Int J Neuropsychopharmacol 2005;8:143-4.

10. Rosen RC, Lane RM, Menza M. Effects of SSRIs on sexual function: a critical review. J Clin Psychopharmacol 1999;19:67-85.

11. Coupland NJ, Bell CJ, Potokar JP. Serotonin reuptake inhibitor withdrawal. J Clin Psychopharmacol 1996;16:356-62.

12. Rosenbaum JF, Fava M, Hoog SL, et al. Selective serotonin reuptake inhibitor discontinuation syndrome: a randomized clinical trial. Biol Psychiatry 1998;44:77-87.

13. Frankle WG, Slifstein M, Hwang DR, et al. Reproducibility of derivation of serotonin transporter parameters with [^{11}C]DASB in healthy humans: comparison of methods. Proceedings of the Society of Nuclear Medicine 50th Annual Meeting, New Orleans, USA, 2003.

Figure legend

Figure 1. Relationship between the plasma concentration of fluvoxamine and mean 5-HT transporter occupancy measured by PET. Measured occupancy was the mean occupancy among five regions (prefrontal cortex, thalamus, striatum, hippocampus, and amygdala).

Psychopharmacology (2006) 185: 395–399
DOI 10.1007/s00213-005-0304-0

ORIGINAL INVESTIGATION

Akihiro Takano · Kazutoshi Suzuki · Jun Kosaka · Miho Ota · Shoko Nozaki · Yoko Ikoma · Shuji Tanada · Tetsuya Suhara

A dose-finding study of duloxetine based on serotonin transporter occupancy

Received: 21 November 2005 / Accepted: 19 December 2005 / Published online: 28 February 2006

Abstract *Rationale:* Positron emission tomography (PET) has been utilized for determining the dosage of antipsychotic drugs. To evaluate the dosage of antidepressants such as selective serotonin reuptake inhibitors, serotonin transporter occupancy (5-HTT) is also a useful index. *Objectives:* We investigated the degree of 5-HTT occupancy with different doses of the antidepressant duloxetine and the time-course of 5-HTT occupancy using PET. *Methods:* PET scans with [^{11}C]DASB were performed before and after a single administration of duloxetine (5–60 mg), and three consecutive scans were performed after a single dose or repeated doses of 60 mg of duloxetine. *Results:* 5-HTT occupancies by duloxetine were increased by 35.3 to 86.5% with dose and plasma concentration increments. The ED_{50} value of 5-HTT occupancy was 7.9 mg for dose and 3.7 ng/ml for plasma concentration. In the time-course of 5-HTT occupancy, mean occupancies were 81.8% at 6 h, 71.9% at 25 h, and 44.9% at 53 h after a single administration, and 84.3% at 6 h, 71.9% at 49 h, and 47.1% at 78 h after repeated administrations. *Conclusions:* Based on 5-HTT occupancy, 40 mg and more of duloxetine was needed to attain 80% occupancy, and 60 mg of duloxetine could maintain a high level of 5-HTT occupancy with a once-a-day administration schedule.

A. Takano · K. Suzuki · J. Kosaka · M. Ota · S. Nozaki · Y. Ikoma · T. Suhara (✉)
Molecular Imaging Center,
National Institute of Radiological Sciences,
9-1, Anagawa 4-Chome, Inage-ku,
Chiba, 263-8555, Japan
e-mail: suhara@nirs.go.jp
Tel.: +81-43-2063194
Fax: +81-43-2530396

S. Tanada
Department of Medical Imaging,
National Institute of Radiological Sciences,
9-1, Anagawa 4-Chome, Inage-ku,
Chiba, 263-8555, Japan

Keywords Duloxetine · Occupancy · 5-HTT · PET · DASB · Time-course

Introduction

Positron emission tomography (PET) studies have made it possible to investigate the in vivo neurotransmission in the living human brain (Farde et al. 1988). Investigations for optimizing the dosage of various CNS drugs based on the relationship between in vivo occupancy and dose/plasma concentration have been reported (Mamo et al. 2004; Andree et al. 2003). The advantage of in vivo receptor occupancy studies using PET was realized from the fact that it revealed inappropriate clinical dose settings of old antipsychotics (Takano et al. 2006). Radio-labeled ligands such as [^{11}C]McN(+)5652 and [^{11}C]DASB have been used to visualize and quantify serotonin transporter (5-HTT) in the brain, and [^{11}C]DASB has relatively higher binding potentials for 5-HTT (Wilson et al. 2000b). Recently, high 5-HTT occupancy by selective serotonin reuptake inhibitors (SSRIs) during the treatment of mood disorder has been reported (Meyer et al. 2001, 2004; Suhara et al. 2003). 5-HTT occupancy was reported to be over 80% at clinical doses of antidepressants such as SSRIs and tricyclic ones during the treatment of depression (Meyer et al. 2001, 2004; Suhara et al. 2003). It was also suggested that investigation of the time-course of receptor occupancy by CNS drugs would help to determine the administration schedule (Tauscher et al. 2002; Takano and Suhara 2005).

Duloxetine is one of the serotonin noradrenaline reuptake inhibitors (Wong 1998), and several double-blind, placebo-controlled clinical trials have demonstrated its efficacy for major depressive disorder (Goldstein et al. 2002; Detke et al. 2004, 2002a,b; Brannan et al. 2005a,b). However, the relationship between dose/plasma concentration and occupancy of the binding site in the brain and the kinetics at the binding site of duloxetine has not been fully explored.

In this study, we investigated the degree of 5-HTT occupancy by different doses of duloxetine and the time-course of 5-HTT occupancy using PET.

Materials and methods

Seventeen healthy male volunteers were enrolled in this study. None had a history of present or past psychiatric, neurological, or somatic disorders, and they had no alcohol- or drug-related problems. They had not taken any kind of medication for at least 1 month before the start of the study. All were nonsmokers. Two volunteers were excluded for PET-related technical reasons. Therefore, 15 healthy male volunteers (24.1+2.4 years old) completed the study. The study was approved by the ethics and radiation safety committees of the National Institute of Radiological Sciences, Chiba, Japan. Written informed consent was obtained from each subject.

Radioligand

[^{11}C]DASB was synthesized by methylation of the corresponding des-methyl precursor with [^{11}C]CH_3I (Wilson et al. 2000a,b). Radiochemical purities were over 95%.

PET studies

The PET study consisted of the two following parts.

Part A: single administration study

Of 15 subjects, 12 subjects participated in the Part A study. Three volunteers each took a single oral dose of 5, 20, 40, or 60 mg of duloxetine. The first PET scan was performed before the duloxetine administration as a baseline study. The second PET scan was performed 6 h after the single-dose administration. A third scan was performed 25 h after administration on the three volunteers taking 60 mg, and this was followed by a fourth scan at 53 h.

Part B: repeated administration study

Three volunteers took 60 mg of duloxetine daily for 7 days. The first PET scan was performed before the duloxetine administration as a baseline study. The second PET scan was performed 6 h after the last administration. Additional scans were performed at 49 and at 78 h after the last administration.

PET procedures

PET scans were carried out with a ECAT 47 (CTI-Siemens, Knoxville, TN, USA) scanner. A head fixation device was used during the scans (Fixter Instruments, Stockholm, Sweden). A 10-min transmission scan was done to correct for attenuation. Dynamic PET scans were carried out for 90 min (1 min×4, 2 min×13, 4 min×5, 8 min×5) in 2-D mode immediately after a bolus injection of 603.8–855.1 (mean±SD, 728.3±47.7) MBq of [^{11}C]DASB with high specific radioactivities (41.1–168.6 GBq/μmol; mean±SD, 98.3±31.5 GBq/μmol).

MRI procedures

T1-weighted images of the brain were obtained by Gyroscan NT (Phillips Medical Systems, Best, The Netherlands) (1.5T).

Plasma concentration of duloxetine

Blood samples were taken to measure the concentrations of duloxetine just before and after each PET scan. The plasma concentrations of duloxetine were determined by LC-MS/MS (Prevalere Life Sciences, NY, USA).

Data analysis

All emission scans were reconstructed with a Ramp filter cutoff frequency of 0.5. The data were not subjected to motion correction. Regions of interest for the thalamus and cerebellum were drawn on the coregistered PET/MRI images using a template-based method (Yasuno et al. 2002).

Quantification was performed using multilinear reference tissue model 2 (Ichise et al. 2003), which was originally developed based on [^{11}C]DASB data. The cerebellum was used as the reference tissue because of its negligible density of 5-HTT. These models allow the estimation of binding potential (BP), which was defined as the ratio of receptor density (B_{max}) to dissociation constant (K_d).

The 5-HTT occupancy was calculated by the following equation:

$$\mathrm{Occu} = \left(\mathrm{BP}_{\mathrm{baseline}} - \mathrm{BP}_{\mathrm{drug}}\right) \times 100/\mathrm{BP}_{\mathrm{baseline}},$$

where Occu is the 5-HTT occupancy, $BP_{baseline}$ is BP in the drug-free state, and BP_{drug} is BP of the subjects with the drug.

The relationship between plasma concentration and 5-HTT occupancy was modeled by the following equation: $\%5\text{–HTT occupancy} = 100 \times C/(ED_{50} + C)$, where %5-HTT occupancy is the percentage of 5-HTT occupied, ED_{50} is a constant, and C is the concentration of the drug in the vicinity of transporters; dose and plasma concentration of duloxetine just before each PET scan were used as functional surrogates of C.

Results

In the Part A study, the 5-HTT occupancies were increased by 35.3 to 86.5% as the dose and plasma concentration of duloxetine were increased (Fig. 1a,b). Mean occupancies were 43.6±8.8% at 5 mg, 71.3±5.3% at 20 mg, 80.6±4.8% at 40 mg, and 81.8±4.3% at 60 mg.

The relationship between plasma concentration of duloxetine and 5-HTT occupancy fitted well at r=0.91, ED_{50}=7.9 mg, r=0.93, ED_{50}=3.7 ng/ml (Fig. 1a,b).

The mean 5-HTT occupancies of three subjects, after taking 60 mg of duloxetine orally, were 81.8±4.3% at 6 hr, 71.9±5.7% at 25 hr, and 44.9±5.3% at 53 hr. The time-courses of mean 5-HTT occupancy and mean plasma concentration of duloxetine of these three subjects are shown in Fig. 2.

In the Part B study, the mean 5-HTT occupancies of three volunteers, after taking 60 mg of duloxetine orally for 7 consecutive days, were 84.3+2.8% at 6 h, 71.9+2.6% at 49 h, and 47.1+3.7% at 78 h (Fig. 3).

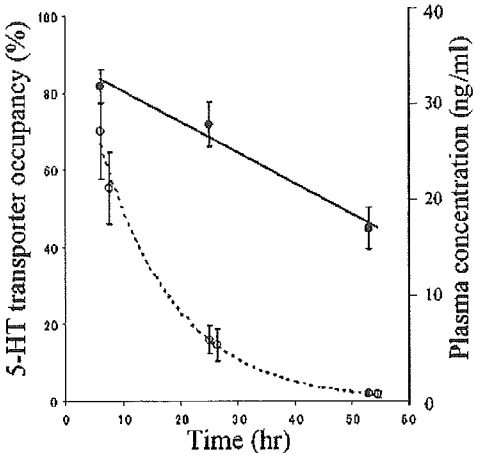

Fig. 2 Time-course of mean plasma concentration of duloxetine (*open circle*) and mean 5-HTT occupancy (*filled circle*) of three volunteers after taking a single dose of 60 mg of duloxetine. The *dotted line* is a one-exponential function fitting the time-course of plasma concentration, and the *solid line* is a linear function fitting the time-course of 5-HTT occupancy

Discussion

The present results showed that 5-HTT occupancy was 80.6±4.8% at 40 mg and 81.8±4.3% at 60 mg of single duloxetine administration. By repeated duloxetine administration, 5-HTT occupancy was 84.3±2.8% at 6 h after last administration. Although the threshold of the clinical effects has not been clearly defined for 5-HTT occupancy, over 80% occupancy was reported by the clinical dose of antidepressants during treatment (Meyer et al. 2001, 2004; Suhara et al. 2003). In this study, more than 40 mg of duloxetine was necessary to attain 80% occupancy and a dosage level comparable to the clinical doses of SSRIs for 5-HTT blockage.

The time-course of 5-HTT occupancy and plasma concentration indicated a relatively high (47.1±3.7% at 78 h after repeated 60-mg administration) occupancy remaining even after the plasma concentration had decreased. From linear fitting to the occupancy time-course, about 70% occupancy was estimated at 24 h after a single administration, and about 78% at 24 h after repeated administrations. Sixty milligrams of duloxetine seems to be the optimal dose for keeping a high 5-HTT occupancy level for extended hours.

Several double-blind, placebo-controlled clinical trials of duloxetine have been performed for major depressive disorder, but the dosage differed among the studies. Eighty milligrams/day (40 mg b.i.d.) and 120 mg /day (60 mg b.i.d.) of duloxetine were reported to show efficacy for major depressive disorder (Goldstein et al. 2002; Detke et al. 2004), and a dose of 60 mg a day was also shown to have a clinical effect in the treatment of major depressive disorder (Brannan et al. 2005a,b; Detke et al. 2002a,b).

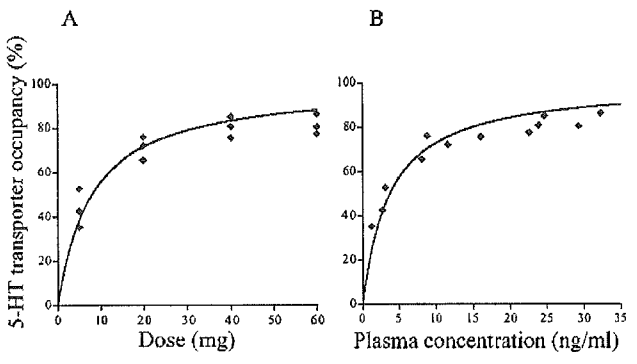

Fig. 1 Relationship between dose (**a**) and plasma concentration (**b**) just before each PET scan of duloxetine and 5-HTT occupancy. The fitting curves were drawn by the following equation: $\%5\text{-}HTToccupancy = 100 \times C/(ED_{50} + C)$, where %5-HTT occupancy is the percentage of 5-HTT occupied, ED_{50} is a constant, and C is the dose and plasma concentration of duloxetine just before each PET scan

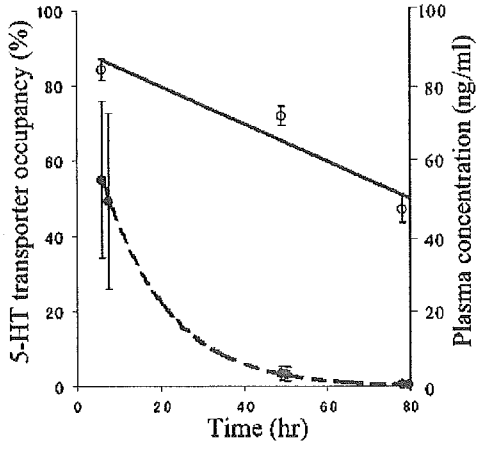

Fig. 3 Time-course of mean plasma concentration of duloxetine (*open circle*) and mean 5-HTT occupancy (*filled circle*) after taking 60 mg of duloxetine daily for 7 days. The *dotted line* is a one-exponential function fitting the time-course of plasma concentration, and the *solid line* is a linear function fitting the time-course of 5-HTT occupancy

Dosage was determined based on a variety of data concerning the plasma pharmacokinetics and brain penetration (Detke et al. 2002a,b; Wong 1998; Yildiz and Sachs 2001), but sufficient objective evidence regarding dosage and administration schedule appeared to be lacking. Our present results would provide some useful objective evidence to assist in defining clinical dosage settings.

Although duloxetine is both a serotonin and noradrenaline transporter reuptake inhibitor, only 5-HTT occupancy was investigated in this study because an adequate PET ligand for noradrenaline transporter is at present not available.

An in vitro report indicated that duloxetine has greater affinity to 5-HTT (Ki=0.8) than to noradrenaline transporter (Ki=7.5)(Bymaster et al. 2001). As in vivo affinity (ED_{50} values) might be estimated from in vitro binding data (Ki values), noradrenaline transporter occupancy by duloxetine would be about 30% at a dose occupying 80% of 5-HTT. Although the in vitro binding data do not always apply to in vivo binding situations, there is a possibility that higher doses may have some effect through higher blockage of noradrenaline transporter (Chalon et al. 2003, Turcotte et al. 2001). The role of noradrenaline reuptake inhibition for duloxetine needs to be clarified.

In this study, the thalamus was used to measure 5-HTT occupancy because it has the highest specific binding in the brain (Houle et al. 2000). We measured 5-HTT occupancy in the thalamus in our previous study with [^{11}C]McN(+)5652 (Suhara et al. 2003), and 5-HTT occupancy has also been reported using [^{11}C]DASB in the thalamus and several other regions (Meyer et al. 2004). Regional differences of 5-HTT occupancy should be discussed in the future.

The cerebellum was used as reference tissue for [^{11}C] DASB quantification (Ginovart et al. 2001; Ichise et al. 2003). Cerebellar gray matter has recently been suggested to be an optimal reference region because it has very low 5-HTT and its effect on binding potential would not to exceed 7% (Kish et al. 2005; Parsey et al. 2006).

Conclusions

We investigated 5-HTT occupancy by duloxetine. It was shown that 5-HTT occupancy increased gradually as dose and plasma concentration increased. Forty milligrams and more of duloxetine was necessary to reach 80% occupancy, a level comparable to the clinical doses of SSRIs regarding 5-HTT blockage. 5-HTT occupancy by 60 mg of duloxetine remained high even after the plasma concentration decreased, and it was observed that this dosage given daily can maintain a high level of 5-HTT occupancy.

Acknowledgement This research was conducted as LY248686 (duloxetine) phase I study in Japan, and was partially supported by Shionogi and Co., Ltd.

References

Andree B, Hedman A, Thorberg SO, Nilsson D, Halldin C, Farde L (2003) Positron emission tomographic analysis of dose-dependent NAD-299 binding to 5-hydroxytryptamine-1A receptors in the human brain. Psychopharmacology (Berl) 167:37–45

Brannan SK, Mallinckrodt CH, Detke MJ, Watkin JG, Tollefson GD (2005a) Onset of action for duloxetine 60 mg once daily: double-blind, placebo-controlled studies. J Psychiatr Res 39:161–172

Brannan SK, Mallinckrodt CH, Brown EB, Wohlreich MM, Watkin JG, Schatzberg AF (2005b) Duloxetine 60 mg once-daily in the treatment of painful physical symptoms in patients with major depressive disorder. J Psychiatr Res 39:43–53

Bymaster FP, Dreshfield-Ahmad LJ, Threlkeld PG, Shaw JL, Thompson L, Nelson DL, Hemrick-Luecke SK, Wong DT (2001) Comparative affinity of duloxetine and venlafaxine for serotonin and norepinephrine transporters in vitro and in vivo, human serotonin receptor subtypes, and other neuronal receptors. Neuropsychopharmacology 25:871–880

Chalon SA, Granier LA, Vandenhende FR, Biek PR, Bymaster FP, Joliat MJ, Hirth C, Potter WZ (2003) Duloxetine increases serotonin and norepinephrine availability in healthy subjects: a double-blind, controlled study. Neuropsychopharmacology 28:1685–1693

Detke MJ, Lu Y, Goldstein DJ, McNamara RK, Demitrack MA (2002a) Duloxetine 60 mg once daily dosing versus placebo in the acute treatment of major depression. J Psychiatr Res 36:383–390

Detke MJ, Lu Y, Goldstein DJ, Hayes JR, Demitrack MA (2002b) Duloxetine, 60 mg once daily, for major depressive disorder: a randomized double-blind placebo-controlled trial. J Clin Psychiatry 63:308–315

Detke MJ, Wiltse CG, Mallinckrodt CH, McNamara RK, Demitrack MA, Bitter I (2004) Duloxetine in the acute and long-term treatment of major depressive disorder: a placebo- and paroxetine-controlled trial. Eur Neuropsychopharmacol 14: 457–470

Farde L, Wiesel FA, Halldin C, Sedvall G (1988) Central D_2-dopamine receptor occupancy in schizophrenic patients treated with antipsychotic drugs. Arch Gen Psychiatry 45:71–76

Ginovart N, Wilson AA, Meyer JH, Hussey D, Houle S (2001) Positron emission tomography quantification of [^{11}C]-DASB binding to the human serotonin transporter: modeling strategies. J Cereb Blood Flow Metab 21:1342–1353

Goldstein DJ, Mallinckrodt C, Lu Y, Demitrack MA (2002) Duloxetine in the treatment of major depressive disorder: a double-blind clinical trial. J Clin Psychiatry 63:225–231

Houle S, Ginovart N, Hussey D, Meyer JH, Wilson AA (2000) Imaging the serotonin transporter with positron emission tomography: initial human studies with [^{11}C]DAPP and [^{11}C] DASB. Eur J Nucl Med 27:1719–1722

Ichise M, Liow JS, Lu JQ, Takano A, Model K, Toyama H, Suhara T, Suzuki K, Innis RB, Carson RE (2003) Linearized reference tissue parametric imaging methods: application to [^{11}C]DASB positron emission tomography studies of the serotonin transporter in human brain. J Cereb Blood Flow Metab 23:1096–1112

Kish SJ, Furukawa Y, Chang LJ, Tong J, Ginovart N, Wilson A, Houle S, Meyer JH (2005) Regional distribution of serotonin transporter protein in postmortem human brain: is the cerebellum a SERT-free brain region? Nucl Med Biol 32:123–128

Mamo D, Sedman E, Tillner J, Sellers EM, Romach MK, Kapur S (2004) EMD 281014, a specific and potent 5HT2 antagonist in humans: a dose-finding PET study. Psychopharmacology (Berl) 175:382–388

Meyer JH, Wilson AA, Ginovart N, Goulding V, Hussey D, Hood K, Houle S (2001) Occupancy of serotonin transporters by paroxetine and citalopram during treatment of depression: a [^{11}C]DASB PET imaging study. Am J Psychiatry 158:1843–1849

Meyer JH, Wilson AA, Sagrati S, Hussey D, Carella A, Potter WZ, Ginovart N, Spencer EP, Cheok A, Houle S (2004) Serotonin transporter occupancy of five selective serotonin reuptake inhibitors at different doses: an [^{11}C]DASB positron emission tomography study. Am J Psychiatry 161:826–835

Parsey RV, Kent JM, Oquendo MA, Richards MC, Pratap M, Cooper TB, Arango V, Mann JJ (2006) Acute occupancy of brain serotonin transporter by sertraline as measured by [^{11}C]DASB and positron emission tomography. Biol Psychiatry (in press)

Suhara T, Takano A, Sudo Y, Ichimiya T, Inoue M, Yasuno F, Ikoma Y, Okubo Y (2003) High levels of serotonin transporter occupancy with low-dose clomipramine in comparative occupancy study with fluvoxamine using positron emission tomography. Arch Gen Psychiatry 60:386–391

Takano A, Suhara T (2005) The necessary parameters for estimating the time-course of receptor occupancy. Int J Neuropsychopharmacol 8:143–144

Takano A, Suhara T, Yasuno F, Suzuki K, Takahashi H, Morimoto T, Lee YJ, Kusuhara H, Sugiyama Y, Okubo Y (2006) The antipsychotic sultopride is overdosed—a PET study of drug-induced receptor occupancy in comparison with sulpiride. Int J Neuropsychopharmacol (in press)

Tauscher J, Jones C, Remington G, Zipursky RB, Kapur S (2002) Significant dissociation of brain and plasma kinetics with antipsychotics. Mol Psychiatry 7:317–321

Turcotte JE, Debonnel G, de Montigny C, Hebert C, Blier P (2001) Assessment of the serotonin and norepinephrine reuptake blocking properties of duloxetine in healthy subjects. Neuropsychopharmacology 24:511–521

Wilson AA, Garcia A, Jin L, Houle S (2000a) Radiotracer synthesis from [^{11}C]-iodomethane: a remarkably simple captive solvent method. Nucl Med Biol 27:529–532

Wilson AA, Ginovart N, Schmidt M, Meyer JH, Threlkeld PG, Houle S (2000b) Novel radiotracers for imaging the serotonin transporter by positron emission tomography: synthesis, radiosynthesis, and in vitro and ex vivo evaluation of ^{11}C-labeled 2-(phenylthio)araalkylamines. J Med Chem 43:3103–3110

Wong DT (1998) Duloxetine (LY248686): an inhibitor of serotonin and noradrenaline uptake and an antidepressant drug candidate. Expert Opin Investig Drugs 7:1691–1699

Yasuno F, Hasnine AH, Suhara T, Ichimiya T, Sudo Y, Inoue M, Takano A, Ou T, Ando T, Toyama H (2002) Template-based method for multiple volumes of interest of human brain PET images. Neuroimage 16:577–586

Yildiz A, Sachs GS (2001) Administration of antidepressants. Single versus split dosing: a meta-analysis. J Affect Disord 66:199–206

0022-3565/06/3162-647–653$20.00
THE JOURNAL OF PHARMACOLOGY AND EXPERIMENTAL THERAPEUTICS

JPET 316:647–653, 2006

Vol. 316, No. 2
88328/3082565
Printed in U.S.A.

In Vivo Evaluation of P-glycoprotein Function at the Blood-Brain Barrier in Nonhuman Primates Using [^{11}C]Verapamil

Young-Joo Lee,[1] Jun Maeda, Hiroyuki Kusuhara, Takashi Okauchi, Motoki Inaji, Yuji Nagai, Shigeru Obayashi, Ryuji Nakao, Kazutoshi Suzuki, Yuichi Sugiyama, and Tetsuya Suhara

The Graduate School of Pharmaceutical Sciences, the University of Tokyo, Bunkyo-ku, Tokyo, Japan (Y.-J. L., H.K., Y.S.); Brain Imaging Project, National Institute of Radiological Sciences, Chiba, Japan (J.M., T.O., M.I., Y.N., S.O., T.S.); and Department of Medical Imaging, National Institute of Radiological Sciences, Chiba, Japan (R.N., K.S.)

Received April 21, 2005; accepted November 16, 2005

ABSTRACT

P-glycoprotein (P-gp) is a major efflux transporter contributing to the efflux of a range of xenobiotic compounds at the blood-brain barrier (BBB). In the present study, we evaluated the P-gp function at the BBB using positron emission tomography (PET) in nonhuman primates. Serial brain PET scans were obtained in three rhesus monkeys after intravenous administration of [^{11}C]verapamil under control and P-gp inhibition conditions ([PSC833 ([3′-keto-Me-Bmt^1]-[Val^2]-cyclosporin) 20 mg/kg/2 h]). The parent [^{11}C]verapamil and its metabolites in plasma were determined by HPLC with a positron detector. The initial brain uptake clearance calculated from the integration plot was used for the quantitative analysis. After intravenous administration, [^{11}C]verapamil was taken up rapidly into the brain (time to reach the peak, 0.58 min). The blood level of [^{11}C]verapamil decreased rapidly, and it underwent metabolism with time. The inhibition of P-gp by PSC833 increased the brain uptake of [^{11}C]verapamil 4.61-fold (0.141 versus 0.651 ml/g brain/min, $p < 0.05$). These results suggest that PET measurement with [^{11}C]verapamil can be used for the evaluation of P-gp function at the BBB in the living brain.

The blood-brain barrier (BBB), formed by brain-capillary endothelial cells, is a functional barrier responsible for restricting the entry of compounds from the circulating blood to the brain parenchyma cells (Reese and Karnovsky, 1967). The highly developed tight junctions between the adjacent brain cerebral endothelial cells are an anatomical feature of the BBB that minimizes the nonspecific penetration of compounds via paracellular route (Pardridge, 1988). In addition to this physical barrier, metabolic enzymes and active efflux transporters on this barrier also play important roles in BBB function. P-glycoprotein (P-gp), a 170-kDa membrane protein that is responsible for the multidrug resistance of tumor cells, is a major efflux transporter contributing to the efflux of a range of xenobiotic compounds in the circulating blood at the BBB (Schinkel et al., 1994; Tamai and Tsuji, 2000; Kusuhara and Sugiyama, 2001; Hirrlinger et al., 2002). Interestingly, P-gp may also be involved in the efflux of β-amyloid and has been suspected to play a role in Alzheimer's disease (Lam et al., 2001; Vogelgesang et al., 2002). In addition, a drug-drug interaction involving P-gp inhibition at the BBB has also been suggested (Sadeque at al., 2000). In a clinical study, when loperamide was administered with quinidine, a known P-gp inhibitor, respiratory depression by loperamide was induced (Sadeque at al., 2000). It is speculated that this is caused by modulation of the P-gp-mediated efflux by quinidine. Furthermore, a genetic polymorphism (C3435T) of P-gp has been reported to be associated with drug resistance in patients with epilepsy (Siddiqui et al., 2003), although a controversial result was reported recently (Tan et al., 2004). Such a genetic polymorphism may be associated with interindividual differences in drug concentration in the central nervous system.

This study was performed through the Advanced and Innovational Research program in Life Sciences from the Ministry of Education, Culture, Sports, Science and Technology, Japan. This work was also partially supported by a research grant from the Society of Japanese Pharmacopoeia and the Minister of Health, Labor and Welfare.

[1] Current affiliation: College of Pharmacy, Kyung Hee University, Seoul, Korea.

Article, publication date, and citation information can be found at http://jpet.aspetjournals.org.
doi:10.1124/jpet.105.088328.

ABBREVIATIONS: BBB, blood-brain barrier; ANOVA, analysis of variance; AUC, area under the curve; C_{max}, maximal concentration; HPLC, high-pressure liquid chromatography; MRI, magnetic resonance image; PET, positron emission tomography; P-gp, P-glycoprotein; PSC833, [3′-keto-Me-Bmt^1]-[Val^2]-cyclosporin; T_{max}, time to reach the C_{max}.

These clinical reports prompted a growing interest in the quantitative evaluation of P-gp function in living human brain.

Recently, in vivo evaluation of P-gp function was proposed using an imaging method with [^{11}C]colchicine, [^{11}C]carvedilol, [^{18}F]paclitaxel, and [^{11}C]verapamil (Elsinga et al., 2004). Hendrikse et al. (1998) demonstrated in rodents that the brain uptake of the P-gp substrate [^{11}C]verapamil was increased after pretreatment with cyclosporin A, a P-gp inhibitor, and they showed that that the distribution volume, estimated by Logan plot, was increased by pretreatment with cyclosporin A (Bart et al., 2003; Elsinga et al., 2004). As for human studies, Sasongko et al. (2005) demonstrated that the ratio of the area under the curve (AUC) of the brain concentration to that of blood concentration was increased in the presence of cyclosporin A, and Kortekaas et al. (2005) reported that the distribution volume of [^{11}C]verapamil in the midbrain was increased in Parkinson's disease patients compared with controls. In the present study, the P-gp function at the BBB was evaluated in rhesus monkeys by PET using [^{11}C]verapamil, with or without a potent P-gp inhibitor PSC833. PSC833 treatment caused a significant increase in the brain uptake clearance of [^{11}C]verapamil, which was determined using integration plot analysis using initial brain and blood concentration data.

Materials and Methods

Chemicals. The P-gp inhibitor PSC833 (Valspodar) was kindly supplied by Novartis (Basel, Switzerland) and was dissolved in Intralipid (Lo et al., 2001) (oil in water emulsion droplet; Otsuka Pharmaceutical, Tokyo, Japan). [^{11}C]Verapamil was synthesized from norverapamil (Eisai Co. Ltd., Tokyo, Japan) as described previously (Wegman et al., 2002) and diluted with approximately 2 to 3 ml 0.9% saline containing 0.75% polyoxyethylenemonosorbitan oleate and 1% ascorbic acid. The specific radioactivity of [^{11}C]verapamil used in all experiments ranged from 28.3 to 79.7 GBq/μmol (47.6 $\pm$ 17.3 GBq/μmol, mean $\pm$ S.D., radiochemical purity is over 95%).

Animals. Three young male rhesus monkeys (Macaca mulatta) weighing approximately 6.0 to 6.7 kg were used. The monkeys were maintained and handled in accordance with recommendations by the United States National Institutes of Health and our own guidelines (National Institute of Radiological Sciences, Chiba, Japan). The study was approved by the Animal Ethics Committee of the National Institute of Radiological Sciences. A magnetic resonance image (MRI) of each monkey brain was obtained beforehand.

PET Scan. All PET scans were performed using a high-resolution SHR-7700 PET camera (Hamamatsu Photonics, Shizuoka, Japan) designed for laboratory animals, which provides 31 transaxial slices 3.6 mm (center-to-center) apart, a 33.1-cm field of view, and spatial resolution of 2.6 mm full width at half-maximum (Watanabe et al., 1997). Monkeys were trained beforehand as being immobilized with the head fixation device to ensure accuracy of repositioning throughout the session (Obayashi et al., 2001). The infusion of PSC833 (20 mg/kg/2 h), a P-gp modulator, or vehicle alone to each monkey was started 1 h before the intravenous administration of [^{11}C]verapamil and maintained during the experiment. After administration of [^{11}C]verapamil, 0.9% saline was flushed into the catheter line to prevent adsorption or retention of verapamil. Arterial blood sampling (~0.5–1.5 ml) was performed via an indwelling arterial port from the saphenous artery at 10 s, 20 s, 30 s, 45 s, 1 min, 1.5 min, 3 min, 4.5 min, 6 min, 8 min, 10 min, 15 min, 20 min, 30 min, 45 min, and 60 min after administration, and the radioactivity in the blood was counted in a well-type γ-scintillation counter. Radioactivity was corrected for decay. After transmission scans for attenuation correction for 30 min, a dynamic emission scan in enhanced 2D mode was performed for 60 min (10 $\times$ 12 s, 30 $\times$ 6 s, 1 $\times$ 5 min, 2 $\times$ 5 min, and 5 $\times$ 8 min; a total of 36 frames). [^{11}C]Verapamil was administered via the saphenous vein as a single bolus at the start of the emission scan. The injected doses of [^{11}C]verapamil were 65.8 $\pm$ 11.5 MBq/kg (mean $\pm$ S.D.). The PET scans were separated by at least 4-week intervals and randomized for each monkey.

Metabolite Analysis. Arterial blood samples were collected at 1, 3, 6, 10, 15, 30, and 60 min after administration of [^{11}C]verapamil. Plasma was obtained by centrifugation and deproteinized with 2 volumes of acetonitrile. The supernatant was analyzed for radioactive components using a high-pressure liquid chromatography (HPLC) system (PU-610A series; GL Sciences, Torrance, CA) with a coupled NaI(Tl) positron detector (Takei et al., 2001) to measure [^{11}C]verapamil metabolites. Isocratic elution was performed with a reversed-phase semipreparative μ-Bondpak C18 column (7.8 $\times$ 300 mm i.d.; Waters, Milford, MA). The mobile phase consisted of a mixture of acetonitrile and 0.1 M ammonium acetate (70:30 v/v). The flow rate was 5 ml/min, and the injected sample size was 1.0 ml. The elute was monitored by ultraviolet absorbance at 254 nm and coupled NaI(Tl) positron detection. The percentage of parent radioactivity was determined from the activity of the parent verapamil with respect to the ^{11}C radioactivity in the chromatogram.

PET Data Analysis. All emission scan images were reconstructed with a 4.0-mm Hann filter, and regions of interest were placed on the whole cerebrum using PET Analyzer (in-house software, National Institute of Radiological Sciences; Maeda et al., 2001), and MRI information on each monkey. The summation images of [^{11}C]verapamil from 0 to 5 min were coregistered on the magnetic resonance images by means of statistical parametric mapping (SPM 2; Welcome Department of Cognitive Neurology, London, UK), and then the volume images were processed with Virtual Place TM (AZE Ltd. Tokyo, Japan). The decay-corrected ^{11}C radioactivity was normalized to the injected dose (% dose). The maximal ^{11}C radioactivity in the cerebrum (C_{max_cereb}) and the time to reach the C_{max_cereb} (T_{max_cereb}) were obtained from the time-^{11}C radioactivity data. The AUC was calculated for brain and blood, and it was calculated using data from 0 to 4.5 min after administration to minimize the bias by metabolites.

Integration Plot. The initial brain uptake was measured over a short period (~1–4.5 min) using integration plot method. The uptake rate of [^{11}C]verapamil can be described by the following equation,

$$\frac{X_{t,cereb}}{C_{t,blood}} = CL_{uptake} \times \frac{AUC_{(0-t)}}{C_{t,blood}} + V_E \quad (1)$$

where CL_{uptake} is the brain uptake clearance based on the blood ^{11}C radioactivity, $X_{t,cereb}$ is the amount of ^{11}C radioactivity in the cerebrum at time t, and $C_{t,blood}$ is the blood concentration calculated from ^{11}C radioactivity. $AUC_{(0-t)}$ represents the area under the blood concentration curve from 0 to t, and V_E represents the initial distribution volume in the brain at time 0. V_E was obtained from the y-intercept of the integration plot and includes the distribution volume in blood residing within the brain as well as the initial distribution volume of [^{11}C]verapamil in the brain rapidly equilibrating with that in blood. Therefore, the CL_{uptake} value can be obtained from the initial slope of a plot of $X_{t,cereb}/C_{t,blood}$ versus $AUC_{(0-t)}/C_{t,blood}$, designated as the integration plot (Kim et al., 1988).

Inhibition of P-gp Function. The effect of PSC833, a P-gp modulator, was evaluated based on the normalized time-activity curves of brain and blood for the three monkeys, with and without PSC833 administration. PSC833 was infused at a dose of 20 mg/kg/2 h starting 1 h before intravenous administration of [^{11}C]verapamil and maintained until the end of the experiment (Song et al., 1999; Rodriguez et al., 2004). In a control experiment, drug vehicle was infused in the same manner. Differences were considered statistically significant when $p < 0.05$ using a one-sided paired t test, with the exception of the time course results in which two-way analysis of variance was used.

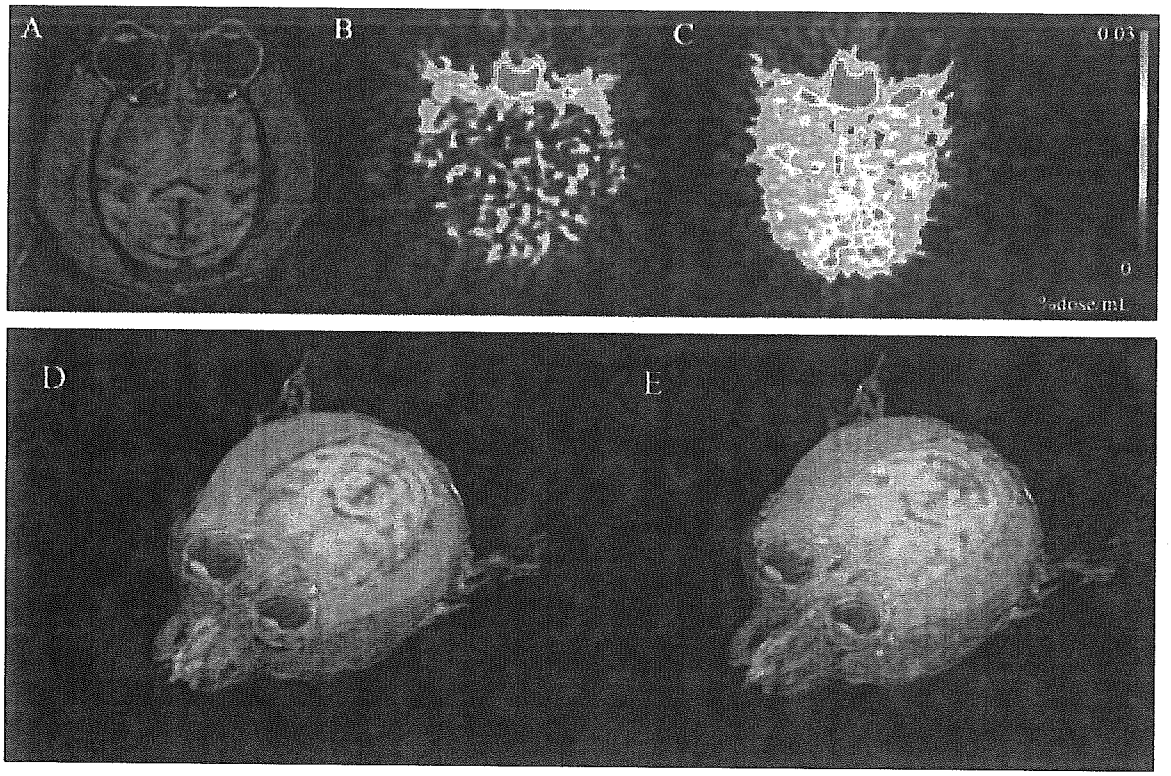

Fig. 1. A typical MRI and a color-coded PET image after administration of [^{11}C]verapamil. Horizontal slices of the brain MRI scans (A) and corresponding summation of PET images (B and C, up to 5 min) of the cerebral ^{11}C radioactivity uptake in one animal. The reconstructed MRI-PET image is also shown to assist intuitive understanding (D and E). B and D represent the control state, and C and E are the P-gp inhibition conditions obtained after PSC833 administration.

Results

The Distribution of [^{11}C]Verapamil in the Brain. A control PET image (Fig. 1B) accompanied by a corresponding morphological MRI (Fig. 1A) showed the uptake of ^{11}C radioactivity in the monkey brain. Higher uptake of ^{11}C radioactivity was observed in the brain after PSC833 treatment (Fig. 1C, PSC833-treated). Brain uptake was also clearly identified from PET/MRI-coregistered images (Fig. 1, D and E). The time-activity curves in the cerebrum are shown in Fig. 2. The ^{11}C radioactivity in the cerebrum peaked at 0.58 min after intravenous administration of [^{11}C]verapamil and remained almost constant at this level up to 60 min. Only limited amount of ^{11}C radioactivity (0.0105 ± 0.0006% dose/g brain, C_{max_cereb}, mean ± S.D.) was transported into the cerebrum.

Treatment with PSC833 significantly increased the ^{11}C radioactivity uptake in the cerebrum (two-way ANOVA, $p < 0.05$). The cerebrum AUC (AUC_{cereb}) of the PSC833 treatment group was significantly greater than that of the control group (1.96-fold) (Table 1; $p < 0.05$). The C_{max_cereb} of the PSC833 treatment group was also significantly higher than that of the control group (1.57-fold) (Table 1, $p < 0.05$). The T_{max_cereb} was not changed by treatment with PSC833 (Table 1).

Blood Profile and Metabolism of [^{11}C]Verapamil. The time-^{11}C radioactivity in the blood is shown in Fig. 3. The ^{11}C radioactivity in the blood fell quickly up to 3 min and then remained constant or slightly increased. Treatment with PSC833 did not affect the blood ^{11}C radioactivity profile (two-way ANOVA). The blood AUC (AUC_{blood}) of the PSC833 treatment group was similar to that of the control group (Table 1).

A chromatogram of the HPLC analysis of [^{11}C]verapamil, with or without treatment with PSC833, is shown in Fig. 4A. The retention time of verapamil was approximately 7 to 8 min. The fraction of intact verapamil decreased with time (Fig. 4B). At 10 min after administration, on average, approximately 25% of the radioactivity in plasma was the metabolite of [^{11}C]verapamil in the control group and intact verapamil represented approximately 50% of the radioactivity in the plasma of the control group 30 min after administration

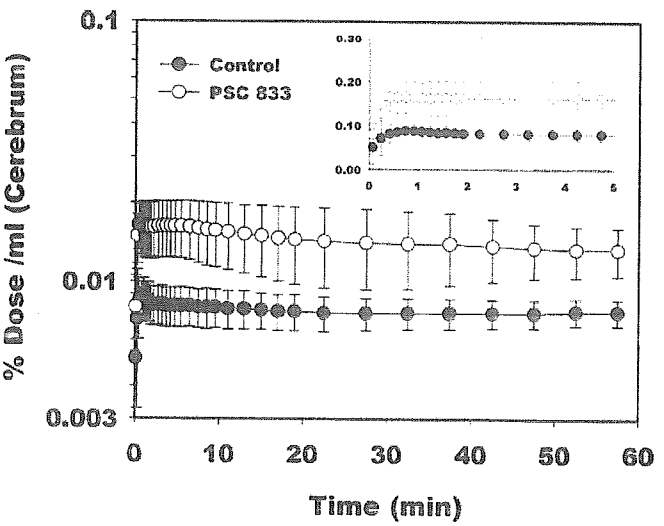

Fig. 2. The ^{11}C radioactivity time curves in cerebrum. The inset shows the detail curves in the early time period (mean ± S.D., $n = 3$). The treatment with PSC833 clearly increases the ^{11}C radioactivity in the cerebrum (two-way ANOVA, $p < 0.05$).

TABLE 1

Pharmacokinetic parameters of [^{11}C]verapamil after intravenous administration, with or without PSC833 (20 mg/kg/2 h)

The AUC_{blood} and AUC_{cereb} were calculated from 0 to 4.5 min after the administration using data shown in Figs. 2 and 3. CL_{uptake} and V_E were obtained from Figure 5. The values represent mean ± S.D. (n = 3). Data in parentheses indicate values from individual animals.

Pharmacokinetic Parameter	Control	+ PSC833 Treatment
AUC_{blood} (% dose × min/ml)	0.0567 ± 0.0145 (0.0461, 0.0733, 0.0507)	0.0535 ± 0.0331 (0.0418, 0.0279, 0.0909)
AUC_{cereb} (% dose × min/g)	0.0365 ± 0.0039 (0.0407, 0.0359, 0.0328)	0.0713 ± 0.0169* (0.0795, 0.0519, 0.0827)
C_{max_cereb} (% dose/g)	0.0105 ± 0.0006 (0.0104, 0.00989, 0.0112)	0.0166 ± 0.0033* (0.0185, 0.0128, 0.0192)
T_{max_cereb} (min)	0.58 ± 0.44 (1.08, 0.42, 0.25)	0.59 ± 0.29 (0.92, 0.42, 0.42)
CL_{uptake} (ml/g/min)	0.141 ± 0.043 (0.185, 0.139, 0.100)	0.651 ± 0.333* (0.937, 0.731, 0.285)
V_E (ml/g)	0.243 ± 0.130 (0.286, 0.0971, 0.346)	0.436 ± 0.279 (0.402, 0.731, 0.176)

* A statistically significant difference was observed (t test, $P < 0.05$).

(Fig. 4B). Treatment with PSC833 slightly increased the metabolite fraction in plasma (Fig. 4B; two-way ANOVA, $p < 0.05$). The inset in Fig. 3 shows the time-activity curves of intact [^{11}C]verapamil in plasma. The plasma radioactivity profile of intact [^{11}C]verapamil was not affected by treatment with PSC833 (two-way ANOVA).

The Brain Uptake Clearance of [^{11}C]Verapamil and Effect of PSC833. Integration plots of the control and PSC833 treatment studies of the three monkeys are shown in Fig. 5, A through C. The integration plots were linear over a short period, which varied from 1 min to 4.5 min, depending on the subject and with or without PSC833 treatment. During this period, the metabolite of [^{11}C]verapamil accounted for less than 12.5% ^{11}C radioactivity. The initial brain uptake of the control group was 0.141 ml/g/min (0.141 ± 0.043, mean ± S.D.), and this was increased after PSC833 treatment (0.651 ± 0.333 ml/g brain/min, mean ± S.D., $p < 0.05$). The V_E was not changed by PSC833 treatment (Table 1). The AUC_{cereb}/AUC_{blood} ratio of ^{11}C radioactivity was increased 2.31-fold in the presence of PSC833.

Discussion

In this study, we evaluated the P-gp function at the BBB in vivo using PET with [^{11}C]verapamil. Recently, the use of imaging techniques, such as single photon emission-computed tomography and PET using [^{11}C]colchicine, [^{11}C]carvedilol, [^{18}F]paclitaxel, and [^{64}Cu]complexes and [^{68}Ga]complexes and [^{99m}Tc]complexes, has been suggested for the noninvasive evaluation of P-gp function in vivo (Elsinga et al., 2004). Among these compounds, [^{11}C]verapamil is a well characterized PET ligand for evaluating P-gp function at the BBB (Hendrikse et al., 1998, 1999), and verapamil can be easily labeled with ^{11}C using commercially available norverapamil (Wegman et al., 2002).

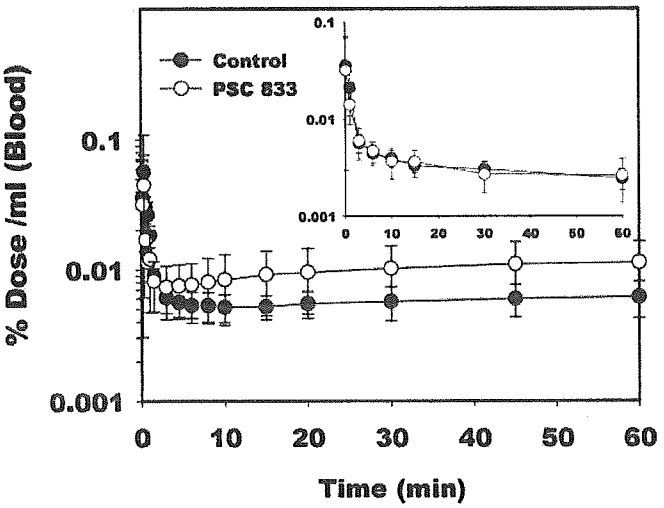

Fig. 3. The [^{11}C]radioactivity and intact (inset) [^{11}C]verapamil activity-time curves in cerebrum and blood. The time-^{11}C radioactivity and intact [^{11}C]verapamil activity curves in blood are similar for both the control and PSC833 treatment groups (mean ± S.D., n = 3).

After intravenous administration of [^{11}C]verapamil, it was rapidly distributed in the brain over a short period and then was eliminated slowly (Fig. 2). Apparently, the ^{11}C radioactivity reached a distributional pseudoequilibrium within a short period (Fig. 3). This is similar to earlier results obtained in rats (Hendrikse et al., 1999). The uptake of ^{11}C radioactivity into the cerebrum increased after PSC833 treatment (Figs. 1 and 2). PSC833 treatment increased the AUC_{cereb} and C_{max_cereb} of ^{11}C radioactivity compared with the values obtained in the control group (Table 1). These data indicate that the efflux transport by P-gp affects the initial brain uptake and that the inhibition of P-gp-mediated transport increases the brain uptake of P-gp substrates (Kusuhara et al., 1997; Dagenais et al., 2000) and supports recent human brain PET study using [^{11}C]verapamil, which was published during the revision process of this manuscript (Sasongko et al., 2005).

The blood concentration-time profile of the ^{11}C radioactivity was biphasic, exhibiting a rapid reduction within minutes followed by an increase in the ^{11}C radioactivity (Fig. 3). The increase at later time points was more marked in the PSC833-treated group than in the control group. The ^{11}C radioactivity in the blood specimens includes unchanged [^{11}C]verapamil and its metabolites (Fig. 4A). Approximately 75% of the ^{11}C radioactivity was unchanged [^{11}C]verapamil during the initial 10 min, and the fraction of the unchanged form in the blood specimens rapidly decreased (Fig. 4B). This observation is consistent with the previous reports of verapamil metabolism in humans (Kroemer et al., 1993; von Richter et al., 2000; von Richter et al., 2001) and monkeys (Link, 2003), whereas low levels of the metabolite of [^{11}C]verapamil during PET studies have been reported in rodents (Hendrikse et al., 1998, 1999). Because the increase at later time points was not observed in the blood concentration-time profile of unchanged [^{11}C]verapamil (Fig. 3, inset), it is likely that the increase is due to the accumulation of metabo-

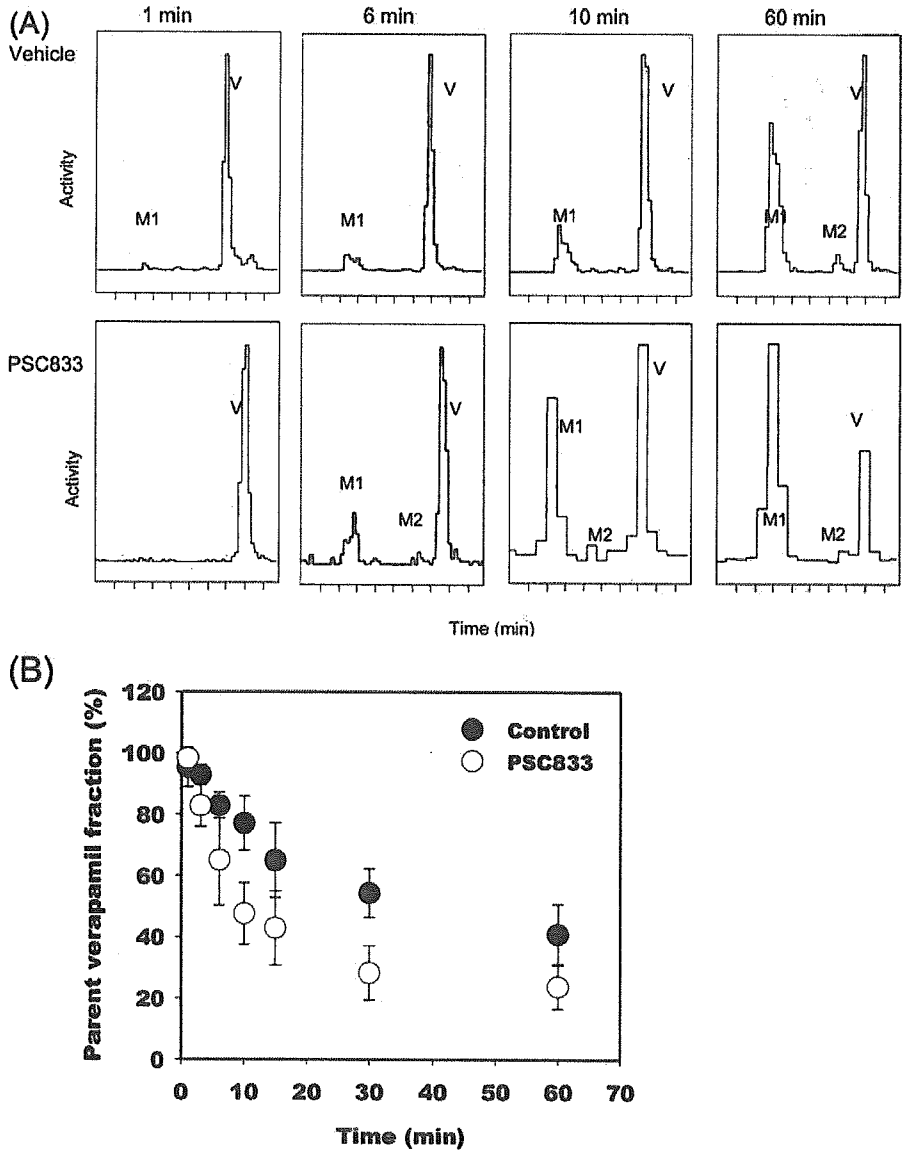

Fig. 4. A, typical chromatograms of plasma samples at 1, 6, 10, and 60 min after intravenous administration of [^{11}C]verapamil, with or without PSC833. B, parent [^{11}C]verapamil fraction of the ^{11}C radioactivity in plasma. The parent verapamil was detected at approximately 7 to 8 min (V). HPLC analysis suggested that there are at least two metabolites (M1, M2) of verapamil after intravenous administration. The parent fraction of verapamil in plasma fell rapidly with time. At 10 min after administration, on average, approximately 75% of the radioactivity in plasma was due to the parent verapamil in the control group and the parent verapamil represented approximately 50% of the radioactivity in the plasma of the control group 30 min after administration (mean ± S.D., n = 3).

lites in the blood from the peripheral tissues. Since PSC833 is known to be a fairly specific P-gp inhibitor with a low degree of metabolic inhibition (Kawahara et al., 2000) and metabolites of verapamil are also substrates of P-gp with a range of specificities (Pauli-Magnus et al., 2000), PSC833 treatment may cause a delay in the elimination of metabolized verapamil, resulting in marked plasma accumulation of metabolites.

Because we could not separate metabolites from parent verapamil in brain, there is a possibility that different parent/metabolite ratio might exist in the brain compared with blood. To deal with this extensive metabolism of [^{11}C]verapamil, we used the initial PET data (~0–4.5min) to avoid any bias from metabolites. Integration plot analysis has been used to obtain a tissue-specific uptake clearance. The initial PET scan data (from 0 to ~1–4.5 min, depending on the subjects) was enough to calculate the initial uptake clearance, during which no extensive metabolism of verapamil was observed (Fig. 4). Figure 5 shows the integration plot of the blood versus tissue time-activity curves in three monkeys (Fig. 5). The CL_{uptake} calculated from the slope of the integration plot increased after treatment with PSC833. This indicates the modulation of P-gp function at the BBB by PSC833 (Table 1) (Kusuhara et al., 1997; Song et al., 1999). The initial brain uptake clearance of [^{11}C]verapamil is a sensitive parameter for P-gp function at the BBB. However, the magnitude of the increase observed in PSC833-treated monkeys was not as high as that observed in P-gp knockout mice. This may be explained by incomplete inhibition of P-gp activity by PSC833, variable brain concentration of PSC833 in monkey, and, partly, a species difference in P-gp expression and/or intrinsic efflux transport activity. In fact, PSC833 treatment does not fully inhibit P-gp function at the BBB in mice (Kusuhara et al., 1997). Interestingly, recent human [^{11}C]verapamil PET study in the presence of cyclosporin A showed a similar degree of increase in the brain distribution of verapamil by P-gp inhibition. In this study, the AUC_{cereb}/AUC_{blood} ratio of ^{11}C radioactivity was increased 1.88-fold in the presence of cyclosporin A, which was consistent with the present study (2.31-fold) (Sasongko et al., 2005). This supports the belief that the species difference in the role of P-gp

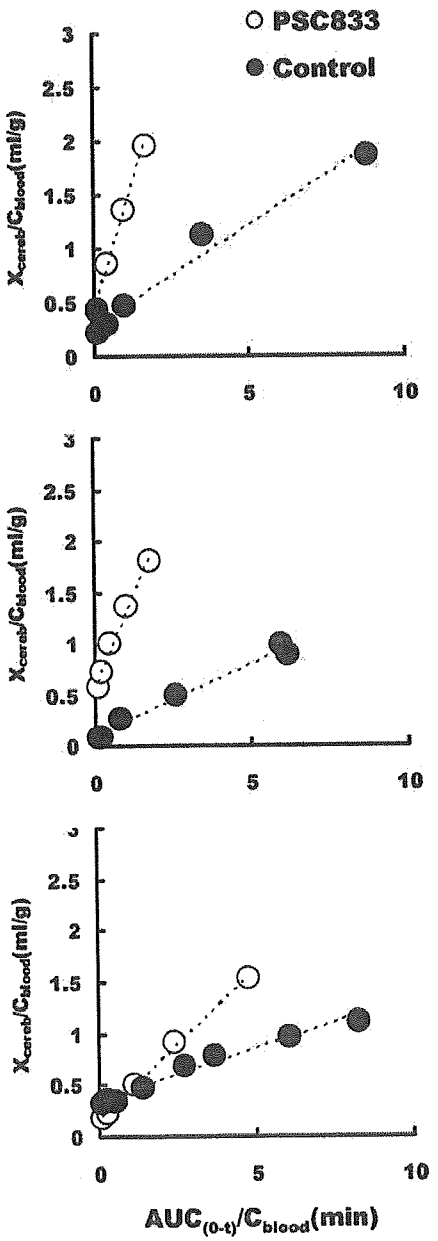

Fig. 5. Integration plot of the brain uptake of [^{11}C]verapamil for the three monkeys (A, B, and C). The initial brain uptake of the control group was increased after treatment with PSC833 (t test, $p < 0.05$, $n = 3$). The V_E was not changed by PSC833 treatment.

at the BBB may not be very significant between humans and monkeys and suggests the feasibility of a PET study using monkeys to provide information on the human BBB. Unlike the slope, the y-intercept of the plot was insensitive to the PSC833 treatment (Table 1). The y-intercept represents the initial distribution volume, including the vascular space and rapid adsorption/binding to the vascular surface, which can achieve rapid equilibrium with the blood compartment. Because the initial distribution volume is greater than the vascular space in the brain, estimated to be 35 μl/g brain in 15 adult rhesus monkeys (Eichling et al., 1975), it seems that the adsorption/binding of [^{11}C]verapamil to the vascular surface occurs within a short period. The use of integration plot analysis helps in the quantitative investigation of P-gp function at the BBB without any interference from the rapid and extensive metabolism of [^{11}C]verapamil, which makes it inappropriate to use common graphical methods that need data obtained from long-term sampling (Logan, 2003).

In conclusion, we have been able to evaluate P-gp function at the BBB in nonhuman primates, using [^{11}C]verapamil as a PET ligand and integration plot method. P-gp at the BBB has attracted much interest from a clinical point of view; i.e., drug-drug interactions and the effects of genetic polymorphisms. Therefore, in future, PET studies using [^{11}C]verapamil will be a powerful tool for evaluating P-gp function at the BBB in a noninvasive manner.

Acknowledgments

We thank the members of the Cyclotron Unit and Radiopharmaceutical and Radiopharmacological Section for operation of the cyclotron and the production of radioisotopes, Novartis Pharm AG for its kind gift of PSC833, and Eisai Co. Ltd. for its kind gift of norverapamil.

References

Bart J, Willemsen AT, Groen HJ, van der Graaf WT, Wegman TD, Vaalburg W, de Vries EG, and Hendrikse NH (2003) Quantitative assessment of P-glycoprotein function in the rat blood-brain barrier by distribution volume of [^{11}C]verapamil measured with PET. *Neuroimage* **20**:1775–1782.

Dagenais C, Rousselle C, Pollack GM, and Scherrmann JM (2000) Development of an in situ mouse brain perfusion model and its application to mdr1a P-glycoprotein-deficient mice. *J Cereb Blood Flow Metab* **20**:381–386.

Eichling JO, Raichle ME, Grubb RL Jr, Larson KB, and Ter-Pogossian MM (1975). In vivo determination of cerebral blood volume with radioactive oxygen-15 in the monkey. *Circ Res* **37**:707–714.

Elsinga PH, Hendrikse NH, Bart J, Vaalburg W, and van Waarde A (2004) PET studies on P-glycoprotein function in the blood-brain barrier: how it affects uptake and binding of drugs within the CNS. *Curr Pharm Des* **10**:1493–1503.

Hendrikse N, Schinkel A, de Vries E, Fluks E, Van der Graaf W, Willemsen A, Vaalburg W, and Franssen E (1998) Complete in vivo reversal of P-glycoprotein pump function in the blood- brain barrier visualized with positron emission tomography. *Br J Pharmacol* **124**:1413–1418.

Hendrikse NH, de Vries EG, Eriks-Fluks L, van der Graaf WT, Hospers GA, Willemsen AT, Vaalburg W, and Franssen EJ (1999) A new in vivo method to study P-glycoprotein transport in tumors and the blood-brain barrier. *Cancer Res* **59**: 2411–2416.

Hirrlinger J, Konig J, and Dringen R (2002) Expression of mRNAs of multidrug resistance proteins (Mrps) in cultured rat astrocytes, oligodendrocytes, microglial cells and neurones. *J Neurochem* **82**:716–719.

Kawahara I, Kato Y, Suzuki H, Achira M, Ito K, Crespi CL, and Sugiyama Y (2000) Selective inhibition of human cytochrome P450 3A4 by *N*-[2(*R*)-hydroxy-1(*S*)-indanyl]-5-[2(*S*)-(1,1-dimethylethylaminocarbonyl)-4-[(furo[2, 3-b]pyridin-5-yl)methyl]piperazin-1-yl]-4(*S*)-hydroxy-2(*R*)-phenylmethylpentanamide and P-glycoprotein by valspodar in gene transfectant systems. *Drug Metab Dispos* **28**: 1238–1243.

Kim DC, Sugiyama Y, Satoh H, Fuwa T, Iga T, and Hanano M (1988) Kinetic analysis of in vivo receptor-dependent binding of human epidermal growth factor by rat tissues. *J Pharm Sci* **77**:200–207.

Kortekaas R, Leenders KL, van Oostrom JC, Vaalburg W, Bart J, Willemsen AT, and Hendrikse NH (2005) Blood-brain barrier dysfunction in parkinsonian midbrain in vivo. *Ann Neurol* **57**:176–179.

Kroemer HK, Gautier JC, Beaune P, Henderson C, Wolf CR, and Eichelbaum M (1993) Identification of P450 enzymes involved in metabolism of verapamil in humans. *Naunyn-Schmiedeberg's Arch Pharmacol* **348**:332–337.

Kusuhara H and Sugiyama Y (2001) Efflux transport systems for drugs at the blood-brain barrier and blood-cerebrospinal fluid barrier (part 1). *Drug Discov Today* **6**:150–156.

Kusuhara H, Suzuki H, Terasaki T, Kakee A, Lemaire M, and Sugiyama Y (1997) P-glycoprotein mediates the efflux of quinidine across the blood-brain barrier. *J Pharmacol Exp Ther* **283**:574–580.

Lam FC, Liu R, Lu P, Shapiro AB, Renoir JM, Sharom FJ, and Reiner PB (2001) β-Amyloid efflux mediated by p-glycoprotein. *J Neurochem* **76**:1121–1128.

Link JM (2003) PET imaging of in vivo transporter and receptor activity, in *AAPS Workshop on Drug Transport: From the Bench to the Bedside*, Wyndham Peachtree Conference Center, Peachtree City, GA.

Logan J (2003) A review of graphical methods for tracer studies and strategies to reduce bias. *Nucl Med Biol* **30**:833–844.

Lo Y, Liu F, and Cherng J (2001) Effect of PSC 833 liposomes and Intralipid on the transport of epirubicin in Caco-2 cells and rat intestines. *J Control Release* **76**:1–10.

Maeda J, Suhara T, Ogawa M, Okauchi T, Kawabe K, Zhang MR, Semba J, and Suzuki K (2001) In vivo binding properties of [carbonyl-^{11}C]WAY-100635: effect of endogenous serotonin. *Synapse* **40**:122–129.

Obayashi S, Suhara T, Kawabe K, Okauchi T, Maeda J, Akine Y, Onoe H, and Iriki A (2001) Functional brain mapping of monkey tool use. *Neuroimage* **14**:853–861.

Pardridge WM (1988) Recent advances in blood-brain barrier transport. *Annu Rev Pharmacol Toxicol* **28**:25–39.
Pauli-Magnus C, von Richter O, Burk O, Ziegler A, Mettang T, Eichelbaum M, and Fromm MF (2000) Characterization of the major metabolites of verapamil as substrates and inhibitors of P-glycoprotein. *J Pharmacol Exp Ther* **293**:376–382.
Reese TS and Karnovsky MJ (1967) Fine structural localization of a blood-brain barrier to exogenous peroxidase. *J Cell Biol* **34**:207–217.
Rodriguez M, Ortega I, Soengas I, Suarez E, Lukas JC, and Calvo R (2004) Effect of P-glycoprotein inhibition on methadone analgesia and brain distribution in the rat. *J Pharm Pharmacol* **56**:367–374.
Sadeque AJ, Wandel C, He H, Shah S, and Wood AJ (2000) Increased drug delivery to the brain by P-glycoprotein inhibition. *Clin Pharmacol Ther* **68**:231–237.
Sasongko L, Link JM, Muzi M, Mankoff DA, Yang X, Collier AC, Shoner SC, and Unadkat JD (2005) Imaging P-glycoprotein transport activity at the human blood-brain barrier with positron emission tomography. *Clin Pharmacol Ther* **77**:503–514.
Schinkel AH, Smit JJ, van Tellingen O, Beijnen JH, Wagenaar E, van Deemter L, Mol CA, van der Valk MA, Robanus-Maandag EC, te Riele HP, et al. (1994) Disruption of the mouse mdr1a P-glycoprotein gene leads to a deficiency in the blood-brain barrier and to increased sensitivity to drugs. *Cell* **77**:491–502.
Siddiqui A, Kerb R, Weale ME, Brinkmann U, Smith A, Goldstein DB, Wood NW, and Sisodiya SM (2003) Association of multidrug resistance in epilepsy with a polymorphism in the drug-transporter gene ABCB1. *N Engl J Med* **348**:1442–1448.
Song S, Suzuki H, Kawai R, and Sugiyama Y (1999) Effect of PSC 833, a P-glycoprotein modulator, on the disposition of Vincristine and digoxin in rats. *Drug Metab Dispos* **27**:689–694.
Takei M, Kida T, and Suzuki K (2001) Sensitive measurement of positron emitters eluted from HPLC. *Appl Radiat Isot* **55**:229–234.
Tamai I and Tsuji A (2000) Transporter-mediated permeation of drugs across the blood-brain barrier. *J Pharm Sci* **89**:1371–1388.
Tan NC, Heron SE, Scheffer IE, Pelekanos JT, McMahon JM, Vears DF, Mulley JC, and Berkovic SF (2004) Failure to confirm association of a polymorphism in ABCB1 with multidrug-resistant epilepsy. *Neurology* **63**:1090–1092.
Vogelgesang S, Cascorbi I, Schroeder E, Pahnke J, Kroemer HK, Siegmund W, Kunert-Keil C, Walker LC, and Warzok RW (2002) Deposition of Alzheimer's β-amyloid is inversely correlated with P-glycoprotein expression in the brains of elderly non-demented humans. *Pharmacogenetics* **12**:535–541.
von Richter O, Eichelbaum M, Schonberger F, and Hofmann U (2000) Rapid and highly sensitive method for the determination of verapamil, [2H7]verapamil and metabolites in biological fluids by liquid chromatography-mass spectrometry. *J Chromatogr B Biomed Sci Appl* **738**:137–147.
von Richter O, Greiner B, Fromm MF, Fraser R, Omari T, Barclay ML, Dent J, Somogyi AA, and Eichelbaum M (2001) Determination of in vivo absorption, metabolism and transport of drugs by the human intestinal wall and liver with a novel perfusion technique. *Clin Pharmacol Ther* **70**:217–227.
Watanabe M, Okada H, Shimizu K, Omura T, Yoshikawa E, Kosugi T, Mori S, and Yamashita T (1997) A high resolution animal PET scanner using compact PS-PMT detectors. *IEEE Trans Nucl Sci* **44**:1277–1282.
Wegman TD, Maas B, Elsinga PH, and Vaalburg W (2002) An improved method for the preparation of [^{11}C]verapamil. *Appl Radiat Isot* **57**:505–507.

Address correspondence to: Dr. Tetsuya Suhara, Brain Imaging Project, National Institute of Radiological Sciences, 9-1, Anagawa 4-Chome, Inage-ku, Chiba 263-8555, Japan. E-mail: suhara@nirs.go.jp

Available online at www.sciencedirect.com
SCIENCE DIRECT®
ELSEVIER
Life Sciences xx (2006) xxx–xxx
Life Sciences
www.elsevier.com/locate/lifescie

Age-related decline of dopamine synthesis in the living human brain measured by positron emission tomography with L-[β-^{11}C]DOPA

Miho Ota [a,b], Fumihiko Yasuno [a], Hiroshi Ito [a,*], Chie Seki [a], Shoko Nozaki [a], Takashi Asada [c], Tetsuya Suhara [a]

[a] *Clinical Neuroimaging Section, Department of Molecular Neuroimaging, Molecular Imaging Center, National Institute of Radiological Sciences, 4-9-1 Anagawa, Inage-ku, Chiba 263-8555, Japan*

[b] *Comprehensive Human Sciences, Medical Sciences for Control of Pathological Processes, Clinical Neuroscience, University of Tsukuba Graduate School, Tsukuba, Japan*

[c] *Department of Psychiatry, University of Tsukuba, Tsukuba, Japan*

Received 5 December 2005; accepted 15 February 2006

Abstract

Loss of dopamine synthesis in the striatum with normal human aging has been observed in the postmortem brain. To investigate whether there is age-associated change in dopamine synthesis in the extrastriatal brain regions similar to that in the striatum, positron emission tomography studies with ^{11}C-labelled L-DOPA were performed on 21 normal healthy male subjects (age range 20–67 years). Decline in the tissue fraction of gray matter per region of interest was also investigated. The overall uptake rate constant for each region of interest was quantified by the Patlak plot method using the occipital cortex as reference region. Regions of interest were set on the dorsolateral prefrontal cortex, lateral temporal cortex, medial temporal cortex, occipital cortex, parietal cortex, anterior cingulate, thalamus, midbrain, caudate nucleus, and putamen. Test–retest analysis indicated good reproducibility of the overall uptake rate constant. Significant age-related declines of dopamine synthesis were observed in the striatum and extrastriatal regions except midbrain. The decline in the overall uptake rate constant was more prominent than in the tissue fraction of gray matter. These results indicate that the previously demonstrated age-related decline in striatal dopamine synthesis extends to several extrastriatal regions in normal human brain.

Keywords: Aging; Reproducibility; L-[β-^{11}C]DOPA; Positron emission tomography

Introduction

Morphological and neurochemical changes are believed to take place in the human central nervous system during the aging process, which might lead to increased vulnerabiliby to the development of several physiological disturbances and neuro-psychiatric disorders closely related to age (Arranz et al., 1996). Postmortem studies indicated that the level of dopamine synthesis (Kish et al., 1992) and several other endogenous neurotransmitters declines in the human striatum during aging (Kish et al., 1995). To estimate the changes of extrastriatal dopamine synthesis in vivo in the living human brain, positron emission tomography (PET) can be used. The ligand ^{11}C-labelled L-DOPA in the carboxy group (L-[β-^{11}C]DOPA) has been reported to be useful for the quantification of L-DOPA metabolism in the brain (Tedroff et al., 1992). Labelling of L-DOPA with ^{11}C allows study with a molecule identical to endogenous L-DOPA as a tracer. In the present study, we evaluated the reproducibility of PET measurement with L-[β-^{11}C]DOPA and age-related changes in dopamine synthesis.

It is also known from postmortem and in vivo studies that the brain shrinks with age (Good et al., 2001). To compare the change of dopamine synthesis with aging in the cerebral cortices, we also investigated age-related atrophy of cerebral cortices using images of gray matter fraction derived from magnetic resonance imaging (MRI).

* Corresponding author. Tel.: +81 43 206 4702; fax: +81 43 253 0396.
E-mail address: hito@nirs.go.jp (H. Ito).

0024-3205/$ - see front matter © 2006 Elsevier Inc. All rights reserved.
doi:10.1016/j.lfs.2006.02.017

Materials and methods

Subjects

Twenty-one healthy male volunteers, age 20 to 67 years (40.0±15.7, mean±SD), participated in the study, and 7 of them, age 20 to 26 years (22.3±2.1), twice underwent PET scans to assess reproducibility. They had no medical history and no brain abnormalities when examined by MRI. This study was approved by the Ethics and Radiation Safety Committees of the National Institute of Radiological Sciences, Chiba, Japan. All participants gave their written informed consent.

Positron emission tomography study

PET scans were performed using an ECAT EXACT HR+ system (CTI-Siemens, Knoxville, Tennessee, USA) in three-dimensional mode, which provides 63 planes and a 15.5 cm field of view. L-[β-^{11}C]DOPA was synthesized from [^{11}C] carbon dioxide via D,L-[3-^{11}C]alanine as described previously (Bjurling et al., 1990; Sasaki et al., 2000). After a 10-min transmission scan with a ^{68}Ge–^{68}Ga source, a bolus of 258–392 MBq of L-[β-^{11}C]DOPA was injected with specific radioactivity of 12.2 GBq/μmol to 81.1 GBq/μmol at the time of injection into the antecubital vein with a 20-ml saline flush. Dynamic PET scanning was started simultaneously with the tracer injection and continued for 60 min (Gefvert et al., 2003). Twenty-three time frames (length: 0.5, 1, 2, 3, 4, or 5 min) were collected. All emission scans were reconstructed with a Hanning filter with a cut-off frequency of 0.4 (full width at half maximum (FWHM)=7.5 mm).

Regions of interest (ROIs) were placed manually on 10 regions (dorsolateral prefrontal cortex, lateral temporal cortex, medial temporal cortex, occipital cortex, parietal cortex, anterior cingulate, thalamus, midbrain, caudate nucleus, and putamen) of the T1-weighted image that had been resliced and coregistered to the PET summation image (0–60 min) individually using SPM2 (Friston et al., 1995). Brain structures were also ascertained by human brain atlas (Mai et al., 1997). Then, time–activity curves of the 10 brain regions were obtained.

For test–retest analysis, seven subjects each underwent two PET scans. The intervals between the test and retest scans were 3 weeks or less. Since it is known that dopamine activity in plasma follows a circadian rhythm (Markianos and Lykouras, 1981), the test–retest studies were performed at the same time of the day.

Magnetic resonance imaging study

T1-weighted images of the brain were obtained from all subjects with a Philips Intera, 1.5 T (Philips Medical Systems, Best, The Netherlands). Scan parameters were 1-mm thick 3 D T1 images with a transverse plane (repetition time, TR/echo time, TE 21/9.2 ms, flip angle 30°, matrix 256×256, field of view (FOV) 256×256), yielding 196 contiguous slices through the head.

PET data analysis

The overall uptake rate constant (K) that quantifies dopamine synthesis was calculated using the graphical analysis developed by Patlak et al. (Patlak and Blasberg, 1985). This analytical method was developed for irreversible ligands and allows for the calculation of K using time–activity data in a reference brain region with no irreversible binding. K values can be estimated by simple linear least squares fitting as follows:

$$\frac{C_i(t)}{C_i'(t)} = K\frac{\int_0^t C_i'(\tau)d\tau}{C_t'} + F_{t>t*}$$

where C_i is the total radioactivity concentration in a brain region, which can be measured by PET; C_i' is the total radioactivity concentration in a brain region with no irreversible compartments; t^* is the equilibrium time of the compartment for unchanged radioligand in the brain tissue. Plotting $C_i(t)/C_i'(t)$ versus $\int_0^t C_i'(\tau)d\tau/C_i'(t)$, after a time t^* yields a straight line with the slope K and intercept F. In the present study, the occipital cortex was used as a region with no irreversible compartments (Torstenson et al., 1997). A range of equilibrium time t^* of 31.5 to 61.5 min was used.

MRI data analysis

Gray matter, white matter, and cerebrospinal fluid images were segmented and extracted from registered MR images using SPM99 (Friston et al., 1995). These segmented MR images provide the tissue fractions of gray and white matter and fraction of cerebrospinal fluid per pixel (ml/ml) (Ito et al., 2005). All gray matter images were smoothed with an isotropic Gaussian kernel at 8-mm FWHM, the same as the FWHM of the PET scanner. Gray matter fraction was obtained from tissue fraction images of gray matter. ROIs used for PET data analysis were drawn on the tissue fraction image of gray matter. ROIs were defined for the dorsolateral prefrontal, lateral temporal, parietal, occipital cortices, anterior cingulate and medial temporal cortex.

Statistics

Statistical analyses were performed with SPSS for Windows 11.0.1.j (SPSS Inc, 1989–2001). The relationship between age and K was evaluated by Pearson's correlation method. For correlation analysis, a p value <0.005 (=0.05/9) was considered significant to avoid type errors in the multiplicity of statistical analysis. The relationship between age and tissue fractions of gray matter was also evaluated by Pearson's correlation method. For correlation analysis, a p value <0.017 (0.05/3) was considered significant.

Reproducibility was assessed in terms of variability and reliability. Within-subject variability was defined as the absolute value of the difference between the test and retest

Table 1
Reproducility of 11 C-labelled L-DOPA K values in human brain

	DorFro	Tempo	Parie	Mid	Med Temp	ACing	Thal	Cau	Puta
Test K (min^{-1}) (mean±S.D.)*e3	2.7±0.3	3.4±0.5	2.1±0.5	60.4±0.9	5.7±0.4	4.6±0.6	4.9±0.9	14.6±1.7	16.6±0.7
Retest K (min^{-1}) (mean±S.D.)*e3	2.6±0.5	3.1±0.5	2.0±0.4	6.0±1.0	5.7±0.7	4.6±0.6	4.7±1.0	14.1±1.8	16.5±1.8
Variability	9.4±8.6	10.1±6.3	10.1±6.3	9.2±9.6	8.8±4.1	9.3±7.3	8.8±5.2	7.3±6.5	7.3±2.4
ICC	0.78	0.76	0.87	0.71	0.54	0.58	0.90	0.73	0.51

DorFro, dorsolateral prefrontal cortex; Tempo, lateral temporal cortex; Parie, parietal cortex; Mid, midbrain; Med Temp, medial temporal cortex; ACing, anterior cingulate; Thal, thalamus; Cau, caudate nucleus; Puta, putamen.

measurements expressed as the percentage of the mean value of the two measurements.

$$\text{Variability}(\%) = (\text{test}-\text{retest}) \times 100/\{(\text{test} + \text{retest})/2\}$$

A measure of the reliability was assessed with the intraclass correlation coefficient (ICC) according to the following equation:

$$\text{ICC} = (\text{MSBS}-\text{MSWS})/(\text{MSBS} + [n-1]\text{MSWS})$$

where MSBS is the mean sum of squares between subjects, MSWS is the mean sum of squares within subjects, and n is the number of repeated observations (in this case, $n=2$). This coefficient is an estimate of the reliability of the two sets of measurement and varies from −1 (not reliable) to +1 (perfectly reliable, i.e., identical test and retest measurements).

To confirm that the shape of the time–activity curve in the occipital cortex used as reference region was unchanged during aging, repeated measures ANOVA was performed for time–activity curves in the occipital cortex normalized by the radioactivity injected and the subject's weight.

Results

Test–retest results are summarized in Table 1. The uptake of ^{11}C-labelled L-DOPA was highest in the putamen. Among the extrastriatal regions, K value was highest in the midbrain (mean $K=0.0062$) and lowest in the parietal cortex (0.0020). All K value measurements showed good to excellent reproducibility with high intraclass correlation coefficients (0.51–0.90) and small within-subject variability with no systematic differences in K values between test and retest (7.3–10.3%).

Repeated measures ANOVA was used to compare radioactivity of the occipital cortex, adjusted for injected dose and weight, among 5 different generation groups (20–29 years old, 30–39, 40–49, 50–59, 60–67) across the 4 frames (31.5, 41.5, 51.5, 61.5 min). There was no significant interaction of group × frame ($F_{12,\ 48}=0.45$; $p=0.94$). Time–activity curves in the occipital cortex did not differ significantly according to age.

The K value of L-[β-^{11}C]DOPA showed a significant negative correlation with age in the dorsolateral prefrontal cortex, lateral temporal cortex, parietal cortex, anterior cingulate, thalamus, medial temporal cortex, caudate nucleus, and putamen, but not in the midbrain (Table 2 and Fig. 1). When linear regression was applied to fit the data, the decrease in K was 16.4% per decade in the dorsolateral prefrontal cortex, 13.8% in lateral temporal cortex, 16.2% in parietal cortex, 8.4% in medial temporal cortex, 13.7% in anterior cingulate, 10.7% in thalamus, 5.4% in caudate nucleus, and 4.2% in putamen.

The tissue fractions of gray matter showed significant negative correlations with age in the cerebral cortex and anterior cingulate (Table 3), with decreases of 3.2% and 2.8% per decade, respectively.

Discussion

We demonstrated very small within-subject variability and high ICC. ROI-based analysis revealed variability of 7.3–10.1% and ICC of 0.51–0.90 for the regions. ICC has often been used as a measure of reliability, with values between 0.4 and 0.75 regarded as fair to good reliability, and greater than 0.9 as excellent (Fleiss, 1986). This criterion also supports the accuracy of the test–retest reliability of L-[β-^{11}C]DOPA measurement of these regions. Regional distribution of K value in the brain also corresponds well with postmortem studies of the distribution of aromatic L-amino acid decarboxylase (AADC) (Lloyd and Hornykiewicz, 1972).

In the human brain, significant losses over a normal life span have been reported for dopamine transporters (Volkow

Table 2
Associations of age and K analyzed using Pearson's correlation coefficients

	DorFro	Tempo	Parie	Mid	Med Temp	ACing	Thal	Cau	Puta
Correlation coefficients	−0.75	−0.65	−0.69	−0.24	−0.69	−0.65	−0.62	−0.60	−0.62
p value	<0.001	0.002	<0.001	0.289	0.001	0.001	0.003	0.004	0.003

DorFro, dorsolateral prefrontal cortex; Tempo, lateral temporal cortex; Parie, parietal cortex; Mid, midbrain; Med Temp, medial temporal cortex; ACing, anterior cingulate; Thal, thalamus; Cau, caudate nucleus; Puta, putamen.